J Biol Phys (2015) 41:117–133
DOI 10.1007/s10867-014-9369-5

ORIGINAL PAPER

Stabilization of Microtubules by Taxane Diterpenoids: Insight from Docking and MD simulations

Umesh Yadava · Hariom Gupta · Mihir Roychoudhury

Received: 12 August 2014 / Accepted: 3 November 2014 / Published online: 27 December 2014

Abstract Microtubules are formed from the molecules of tubulin, whose dynamics is important for many functions in a cell, the most dramatic of which is mitosis. Taxol is known to interact within a specific site on tubulin and also believed to block cell-cycle progression during mitosis by binding to and stabilizing microtubules. Along with the tremendous potential that taxol has shown as an anticancer drug, clinical problems exist with solubility, toxicity, and development of drug resistance. The crystal structure of taxane diterpenoids, namely, 10, 13-deacetyl-abeo-baccatin-IV (I), 5-acetyl-2-deacetoxydecinnamoyl-taxinine-0.29hydrate (II), 7, 9-dideacetyltaxayuntin (III), and Taxawallin-K (IV), are very similar to the taxol molecule. Considerable attention has been given to such molecules whose archetype is taxol but do not posses long aliphatic chains, to be developed as a substitute for taxol with fewer side effects. In the present work, the molecular docking of these taxane diterpenoids has been carried out with the tubulin alpha-beta dimer (1TUB) and refined microtubule structure (1JFF) using Glide-XP, in order to assess the potential of tubulin binding of these cytotoxic agents. Results show that all the ligands dock into the classical taxol binding site of tubulin. Taxol shows the best binding capabilities. On the basis of docking energy and interactions, apart from taxol, molecule II has a better tendency of binding with 1TUB while molecule I shows better binding capability with bovine tubulin 1JFF. To validate the binding capabilities, molecular dynamics (MD) simulations of the best docked complexes of ligands with 1JFF have been carried out for 15.0 ns using DESMOND. Average RMSD variations and time line study of interactions and contacts indicate that these complexes remain stable during the course of the dynamics. However, taxol and molecule II prevail over other taxoids.

Keywords Tubulin binding · Taxane diterpenoids · Molecular docking · Molecular dynamics

1 Introduction

Microtubules are formed from the molecules of tubulin, each of which is a heterodimer consisting of closely related and tightly linked globular polypeptides called α-tubulin and β-

Electronic supplementary material The online version of this article (doi:10.1007/s10867-014-9369-5) contains supplementary material, which is available to authorized users.

U. Yadava (✉) · H. Gupta · M. Roychoudhury
Department of Physics, DDU Gorakhpur University, Gorakhpur 273009, India
e-mail: u_yadava@yahoo.com

tubulin. Its dynamics is important for many functions in a cell, the most dramatic of which is mitosis. Considerable interest has been given to the search and the development of novel small molecules that affect the tubulin polymerization [1]. The chemotherapeutic drug taxol (TXL) is known to interact within a specific site on β-tubulin [2]. It is used clinically in the treatment of ovarian cancer, small cell lung cancer, metastatic breast disease, and other manifestations of the affliction. Taxol is believed to block cell-cycle progression during mitosis by binding to and stabilizing microtubules [3]. Along with the tremendous potential that taxol has shown as an anticancer drug, clinical problems exist with solubility, toxicity, and development of drug resistance, etc. [4]. Several side effects such as a reduction in WBC and RBC, hair loss, nausea and vomiting, hypersensitivity, shortness of breath, low blood pressure, etc., are also caused by this anticancer drug.

Over the past decade, extensive attention has been paid to taxane diterpenoids, whose prototype is taxol [5]. The crystal structure of taxane diterpenoids, namely, 5-acetyl-2-deacetoxydecinnamoyl-taxinine-0.29hydrate (I) and 10,13-deacetyl-abeo-baccatin-IV (II), isolated from the needles and heartwood, respectively, of the *Taxus Wallichiana*, were reported by us [6, 7]. Induced-fit docking studies demonstrated that these compounds I and II may exhibit anti-inflammatory properties and inhibition of anti-coagulation activities of phospholipase A_2 [8]. The structure of the diterpenoid molecules I and II are similar to the taxol molecule except for the substitution of the long aliphatic side chain by−OH and others by keto groups. Two other known taxane diterpenoids, namely, 7,9-dideacetyltaxayuntin (III) and Taxawallin-K (IV), isolated from *Taxus Wallichiana* Zucc, have similar structures as the molecule II, but they differ in substituents [9]. Molecule III possesses a higher number of hydroxyl substituents whereas IV has less ionizable hydrogens. Crystallographic analysis reveals that these molecules (I-IV) (Fig. 1) form cage-like conformations, which is found to be necessary for binding to tubulin. The hydroxyl groups with these molecules enhance the solubility of the molecules. In the present study, molecular docking studies of these taxane diterpenoids (I-IV) along with TXL have been conducted with the tubulin alpha-beta dimer [10] and refined microtubule structure [11] in order to explore the potential of tubulin binding of these cytotoxic agents within the classical taxol binding site of β-tubulin. In order to study the time behavior of the docked complexes, molecular dynamics simulation of 15.0 ns has been carried out on the best docking complexes.

2 Methodology

The three-dimensional crystal structures of tubulin alpha-beta dimer (PDB ID: 1TUB) and refined structure of microtubule (PDB ID: 1JFF), determined by X-ray crystallography, were retrieved from the Protein Databank Bank (http://www.rcsb.org/). Coordinates of the ligand molecules were taken from the reported entries [6, 7, 9] while the coordinates of taxol were extracted from one of the protein complexes (1JFF). The problem of missing residues is corrected using the Prime application while added water, more than one molecule, chain breaks, alternate locations etc. are corrected using protein preparation wizard of the Schrödinger suite [12]. Both 1TUB and 1JFF contain two chains, 'A' and 'B', one of which, containing 'taxol', was retained while the other chain was deleted for the purpose of docking. Ligands GDP, and GTP of 1TUB and GDP, GTP, Zn, and Mg of 1JFF help to crystallize the proteins [10, 11]. These ligands were removed from the structures because they played no critical role in taxol binding. Before docking, the preparations of proteins and ligands were carried out using Protein Preparation and Ligprep Wizards, respectively, of the Suite. Docking studies have been carried out using Glide (Grid-based Ligand Docking with Energetics) [13] in Extra-Precision mode. Glide carries out an exhaustive conformational search, improved by a

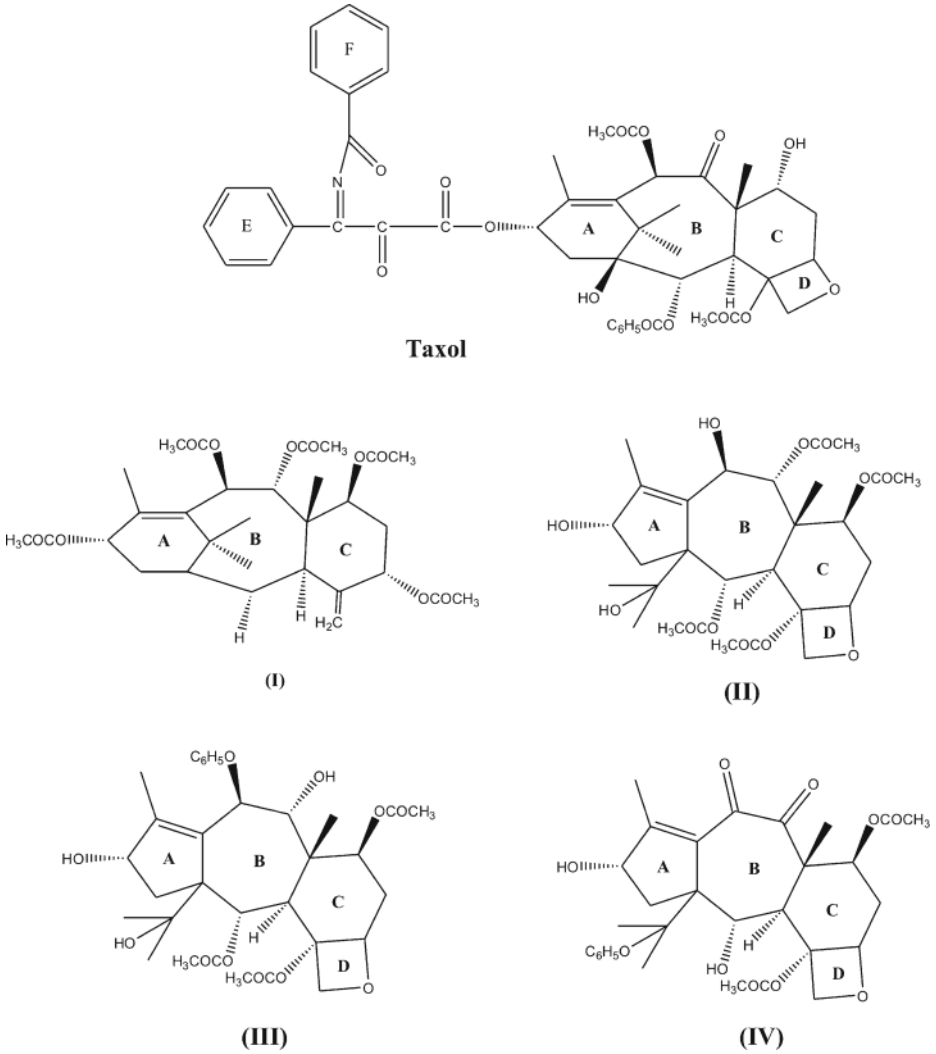

Fig. 1 Chemical structure of taxol and taxane diterpenoids I-IV

heuristic screen that rapidly eliminates conformations deemed not to be suitable for binding to a receptor, such as conformations that have long-range internal hydrogen bonds. During the docking simulation, the ligands were treated as flexible and the receptor was kept rigid, which facilitates the generation of multiple configurations of the receptor–ligand complexes. The docking complexes were ranked by Glide scores (G-scores). The G-score takes into account a number of parameters like hydrogen bonds, hydrophobic contacts, Coulombic, van der Waals, polar interactions in the binding site, metal binding terms and energy penalties for freezing rotatable bonds and buried polar groups. The Extra-Precision (XP) docking protocol of Glide includes protein-ligand structural motifs leading to enhanced binding affinity, in addition to unique water desolvation energy terms [14, 15].

Protein–ligand complexes, retrieved from the RCSB web site, were prepared using the Protein-Preparation Wizard of the Schrödinger Suite, where hydrogens were added and

subsequent refinement of structure was carried out. It was observed that no water molecules were involved in the hydrogen bonding of ligands with proteins in both complexes. Therefore, all the co-crystallized water molecules were removed and bond orders were reassigned. Further, whole systems were minimized to an RMSD of 0.30 Å. Other parameters were taken as reported in our earlier paper [15]. β-tubulin lacks 18 residues in 1TUB, while no missing residue was observed in the β-tubulin of 1JFF. Missing residues were corrected using the Prime module and the Build Panel of the Schrödinger Suite.

All the ligands (TXL and I-IV) were prepared using the Ligprep module of the Schrödinger Suite, which produces structures with various ionization states, tautomers, stereochemistries, and ring conformations. The bond orders were modified according to their data and different conformers were generated. The numbers of conformers generated were 20, 12, 26, 32, and 25, respectively, for molecules TXL, I, II, III, and IV. Each generated conformer was subjected to a full minimization in the gas phase with the Optimized Potential for Liquid Simulations (OPLS2005) all-atom force field [16, 17] to eliminate the bond length and bond angles biased from the crystal structure. OPLS2005 allows proper treatment of metals and gives almost the same results as OPLS2001. Prepared ligands and receptors were used as the initial coordinates for docking purposes. The first stage of ligand docking is the receptor grid generation for which the complex structures 1TUB and 1JFF were considered. The receptor grid was generated using a 1.0 van der Waals radius scaling factor, 0.25 partial charge cut-off without any constraint [18]. Partial charges for the ligand atoms were obtained from the OPLS-AA force field [19], which do not reflect the influence of the environment on the atomic charges. The location of taxol in both complexes was taken as a binding site for docking of all the ligands. In the minimization of ligands, the distance-dependent dielectric constant with a value of 2.0 and a conjugate gradient algorithm with 1,000 steps have been used. All of the inhibitors were passed through a scaling factor of 0.80 and partial charge cutoff of 0.15. After docking, to improve the geometry of the configurations, post-docking minimizations were performed. Post-docking minimization specifies a full force-field minimization of those configurations which are considered for the final scoring. The docking results were used for binding energy calculations and docking scores [20].

The coordinates of the best docking configurations were subjected to molecular dynamics simulation using DESMOND [21, 22]. A suitable number of Na^+ counter-ions were used to neutralize the complexes. The whole system was immersed in a Monte-Carlo-equilibrated, periodic TIP3P water bath, which extended approximately 10.0 Å in each direction. Model systems were generated using the OPLS2005 force field. The Verlet-leap-frog algorithm [23] was used in numerical integration with a 1.0-fs time step for minimization and 2.0 fs for dynamics. A cut-off of 9.0 Å was applied to the Lennard–Jones interactions and constant pressure was maintained with isotropic molecule-based scaling. Water molecules and counter-ions were first energy-minimized by steepest descent followed by conjugate-gradient energy minimization with a satisfactory convergence of rms gradient of 0.1 kcal/mole-Å. The whole system was subjected to 10,000 steps of steepest-descent minimization followed by conjugate-gradient minimization. The velocities were assigned at 100 K to all the atoms according to Boltzmann's distribution. The temperature of the system was raised from 100 K to 298 K over 2 ps by scaling velocities according to the Berendsen algorithm followed by a constant pressure dynamics run over 25 ps at 298 K. After the initial equilibration, a molecular dynamics production run was carried out for 15.0 ns.

The prediction of ADME (absorption, distribution, metabolism, and excretion) and other pharmaceutically important properties of the ligands have also been accomplished through the QikProp3.5 module [24]. The program predicted 44 properties for all the molecules, consisting of principal descriptors and physiochemical properties including the acceptability of the

analogues based on Lipinski's 'rule of 5' [25] and Jorgensen's 'rule of 3'[26]. The rules describe molecular properties important for drug pharmacokinetics in the human body, including ADME. The toxicity predictions of the ligands were carried out using Tox-tree software [27].

3 Results and Discussion

Molecular modeling studies and X-ray crystallographic coordinates reveal the presence of amino acid residues surrounding and interacting with the taxol binding site of the β-tubulin, where molecular docking of four taxoids (I-IV) and the crystallographic ligand taxol (TXL) (Fig. 1) have been conducted. The results of Glide docking with 1TUB and 1JFF for the best docked configurations are presented in Tables 1 and 2, respectively. Table 3, and Figs. 2 and 3 depict the interactions of the ligands with tubulin in the best docking configurations. The outcome of docking studies of each ligand within the classical tubulin binding sites of targets 1JFF and 1TUB are presented here.

Table 1 Van der Waals, Coulomb, Glide energies, and Glide scores of the best five docked configurations of ligands complexed within the active site of 1TUB

Molecules XP_1TUB	Entry ID	E_{vdw} (kcal/mol)	E_{coul} (kcal/mol)	XP_Hbond (kcal/mol)	Glide energy (kcal/mol)	Glide score (kcal/mol)
TXL	2	−50.742	−17.070	−6.524	−67.812	−11.457
	3	−62.771	−12.273	−4.796	−75.044	−11.388
	4	−49.154	−15.641	−5.102	−64.796	−11.376
	5	−42.541	−18.190	−5.496	−60.730	−11.000
	6	−63.640	−12.364	−4.785	−76.004	−10.944
I	37	−38.409	−15.196	−3.840	−54.312	−8.633
	46	−40.854	−10.740	−3.483	−51.324	−8.187
	61	−40.429	−11.827	−2.991	−52.255	−7.913
	62	−29.342	−10.790	−3.914	−40.132	−7.894
	67	−46.455	−9.696	−3.289	−56.152	−7.786
II	27	−39.827	−17.041	−4.333	−56.868	−8.980
	28	−32.732	−15.503	−4.847	−48.235	−8.939
	29	−41.981	−16.321	−4.029	−58.302	−8.892
	31	−45.321	−12.351	−4.064	−57.672	−8.763
	32	−30.281	−19.072	−4.907	−49.353	−8.754
III	40	−39.822	−15.938	−3.840	−53.114	−8.402
	44	−44.417	−10.933	−2.733	−55.411	−8.302
	53	−37.651	−6.594	−4.340	−44.245	−8.043
	55	−38.371	−13.911	−4.077	−52.282	−8.024
	56	−32.881	−8.881	−4.460	−41.761	−7.995
IV	26	−30.654	−15.127	−4.435	−45.781	−8.986
	36	−30.819	−15.196	−3.900	−46.015	−8.640
	42	−35.170	−20.082	−3.943	−55.251	−8.351
	51	−30.806	−9.549	−3.545	−40.355	−8.071
	69	−34.047	−10.006	−3.343	−44.053	−7.771

Table 2 Van der Waals, Coulomb, Glide energies, and Glide scores of the best five docked configurations of ligands complexed within the active site of 1JFF

Molecules XP_1JFF	Entry ID	E_{coul} (kcal/mol)	E_{vdw} (kcal/mol)	XP_Hbond (kcal/mol)	Glide energy (kcal/mol)	Glide score (kcal/mol)
TXL	2	−21.561	−50.704	−5.679	−72.265	−13.213
	3	−17.823	−57.696	−5.675	−75.519	−12.410
	4	−16.617	−48.912	−6.551	−65.529	−12.249
	5	−20.063	−58.461	−5.918	−78.524	−11.963
	6	−16.753	−62.965	−5.736	−79.718	−11.925
I	51	−8.737	−32.992	−3.360	−41.729	−7.800
	53	−4.839	−36.969	−3.858	−41.808	−7.774
	60	−10.322	−33.839	−3.799	−44.161	−7.611
	68	−10.992	−32.916	−3.360	−43.909	−7.421
	76	−9.886	−37.225	−2.880	−47.111	−7.342
II	42	−7.262	−35.251	−4.407	−42.513	−8.158
	54	−12.079	−36.535	−4.168	−48.614	−7.771
	55	−14.398	−32.347	−3.953	−46.746	−7.755
	62	−8.215	−36.853	−3.635	−45.069	−7.590
	66	−9.262	−31.662	−3.840	−40.924	−7.480
III	44	−4.873	−44.928	−2.880	−49.800	−8.046
	64	−9.576	−30.973	−2.933	−40.549	−7.579
	65	−8.012	−37.189	−4.032	−45.201	−7.550
	69	−5.568	−36.862	−3.840	−42.430	−7.419
	72	−9.494	−38.217	−3.840	−47.712	−7.382
IV	36	−10.944	−29.972	−4.000	−40.916	−8.500
	38	−10.630	−27.024	−4.169	−37.655	−8.334
	46	−8.039	−29.926	−3.631	−37.965	−8.026
	49	−10.852	−28.604	−4.153	−39.457	−7.955
	59	−12.522	−20.947	−3.920	−39.457	−7.628

3.1 Docking of ligands with αβ- tubulin dimer (1TUB)

The structure analysis of 1TUB reveals that the constituent α- and β-tubulins of microtubules are basically identical. Each constituent monomer consists of a core of two β sheets surrounded by α-helices, which can be divided into three functional domains: a C-terminal domain, which almost entirely constitutes the binding surface for motor proteins, the N-terminal domain containing the nucleotide-binding region, and an intermediate domain containing the taxol-binding site. The main binding site of taxol resides in the β-subunit near the top of helix H1 (that is, between 15 and 25), and near H5 and the H5–H6 loop (that is, between 212 and 222). The main interaction of the taxane ring with tubulin is at L275, at the beginning of the B8–H9 loop [10].

The various energies of the five best configurations of the docked complexes of taxoids with 1TUB, as obtained through XP docking of Glide, are summarized in Table 1. The five best docked configurations were selected on the basis of better docking scores, better Glide energies, and lower RMSDs [28]. TXL has the best docking score as well as

Table 3 Hydrogen bonding interactions in the docking complexes of the compounds with 1JFF and 1TUB

Molecule	Binding energy (kcal/ mol)	Hydrogen Bonding (D_H…A)	d(H…A) (Å)	Angle (D-H…A) (◦)
Docking complexes with 1TUB				
TXL	-67.947	(LIG) O-H…O(THR276)	2.045	155.4
		(LIG) O-H…N(HIS229)	1.873	170.8
		(LIG) O-H…O(ASP226)	1.796	172.4
I	-54.312	(LIG) O-H…N(HIS229)	2.075	168.4
		(HIE229) N-H…O(LIG)	1.958	168.4
		(LIG) O-H…N(HIS229)	1.768	167.6
		(LIG) O-H…O(ASP26)	1.709	167.2
II	-58.302	(LIG) O-H…O(ASP226)	1.679	169.0
		(LIG) O-H…O(SER232)	1.883	161.3
		(HIS229) N-H…O(LIG)	1.730	140.5
		(LIG) O-H…O (THR276)	2.222	156.0
III	-53.114	(LIG) O-H…O(ASP26)	1.894	172.4
		(LIG) O-H…O(GLY370)	1.878	161.0
		(LIG) O-H…O(THR276)	1.957	157.6
IV	-55.251	(LIG) O-H…O(ASP226)	1.720	171.3
		(LIG) O-H…O(GLY370)	2.144	155.1
Docking complexes with 1JFF				
TXL	-79.718	(LIG) O-H…O(ARG278)	1.860	170.8
		(LIG) O-H…O(THR276)	1.866	171.1
		(LIG) O-H…O(PRO274)	2.175	148.9
		(LIG) O-H…O(ASP26)	2.131	158.9
		(LIG) N-H…O(ASP26)	1.778	122.7
		(GLY370) N-H…O(LIG)	2.317	162.7
I	-44.161	(LIG) O-H…O(THR276)	1.938	158.2
		(LIG) O-H…N(HIS229)	2.077	151.0
II	-55.051	(THR276) N-H…O(LIG)	1.910	149.4
		(LIG) O-H…O(PRO274)	2.123	155.9
		(LIG) O-H…N(HIS229)	2.090	167.0
III	-40.549	(LIG) O-H…O(HIS229)	1.961	152.9
		(LIG) O-H…O(THR276)	1.855	154.9
		(GLY370) N-H…O(LIG)	2.436	130.5
IV	-40.916	(LIG)O-H…O(THR276)	1.983	140.6
		(LIG)O-H…O(THR276)	2.106	149.1
		(LIG)O-H…O(PRO274)	2.322	149.8
		(LIG) C-H…N(HIS229)	2.149	121.1
		(LIG)O-H…O(GLY370)	2.324	154.6

the best binding energy. All the molecules I-IV posses nearly the same Glide scores of about −8.0 kcal/mol while TXL has been found to have −11.457 kcal/mol. Molecule IV, which has less ionizable hydrogens, is found to have the second best Glide score,

whereas compound III has the lowest score. These results are in good agreement with the in vitro experimental studies of III, IV, and TXL with cell lines HepG2 and NCL-H226. For their best Glide scores, molecule II has the best Glide energy after TXL, while molecule IV has the lowest. The in vitro anticancer activity for cell lines A498 and MDR 2780 AD also indicates that molecules III, IV, and taxol have similar results [9] as they can be placed on the basis of Glide energy (Table 4). The minimum docked energy, out of 20 docked configurations of taxol binding with 1TUB, was found to be −76.004 kcal/mol, with a Glide score of −10.944 kcal/mol. The second and third best docked energies are −58.302 and −57.672 kcal/mol, shown by compounds I and II, respectively, whose archetype is taxol. The Coulomb energies and van der Waals energies of the complexes are sufficient to stabilize the complex.

In their best configurations, O-H…O and N-H…O type hydrogen bondings are displayed by ligands with diverse residues of the active site of 1TUB (Table 3 and Fig. 2). Classical O-H…O hydrogen bonding interactions are present in the complexes with residue THR276 by molecules TXL, I and III; with ASP226 by TXL, I and IV; with ASP26 by II and III; with GLY370 by III and IV and with SER232 by molecule I. The hydrogen bonding interactions of the type O-H…N are exhibited by TXL, I, and II involving residue HIS229. The study of protein–ligand interactions show that non-covalent π-π or cation-π interactions are absent in all the docking complexes (Fig. S1). There exist polar interactions in the complexes involving residues SER277, THR276, SER232, HIS229, SER236, and GLN281. In addition to these interactions, almost all the ligands form an array of hydrophobic interactions with conserved residues like LEU275, LEU371, PRO360, ALA233, VAL23, PHE272, PRO274, ILE212, LEU227, LEU230, LEU219, CYS213, LEU217, VAL23, LEU275, PHE272, and LEU230 lining the binding region of taxol (Fig. S1).

3.2 Docking of ligands with the refined structure of αβ-tubulin dimer (1JFF)

The refined structure of αβ-tubulin dimer at 3.5Å resolution (1JFF), reported by Lowe et al. [11], has no major change in overall folds of tubulin with respect to the previous structure (1TUB). However, geometry was improved and positions of side chains were much better defined. The molecular docking of the ligands (TXL and I-IV) was further carried out with this refined microtubule structure (1JFF) to study significant changes in interactions.

The docking results indicate that in all cases the major contribution of binding energy comes from van der Waals interactions, as has been shown in the previous case. The cavity energy term is very small, indicating a very low energy penalty for the ligands buried within the cavity. It can be observed from Table 2 that, in the docking with 1JFF, the magnitude of the Glide score for TXL has increased, while scores have slightly decreased for the docking of rest of the ligands. It is noticed that the relative Glide scores of molecules with 1TUB are the same as those with 1JFF. The RMSD of TXL in its best docking configuration from its PDB structure has been found to be 6.604 Å. On the basis of the Glide score, molecule IV attained the second place while II, III, and I are at the third, fourth, and fifth places, respectively. These results are in good agreement with the in-vitro anticancer activity for cell lines HepG2 and NCI-H226 (Table 4). Out of five best score configurations, TXL exhibits the best docking energy −79.718 kcal/mol, which is about 3.0 kcal/mol better than the docking results with 1TUB. Molecules III, II, I and IV exhibit the minimum docking energy values of −49.800, −48.614, −47.111, and −40.916 kcal/mol, respectively.

The hydrogen bonding interactions as observed in the docking complexes with 1JFF are similar to the case of docking with 1TUB (Table 3 and Fig. 4). O-H…O and N-H…

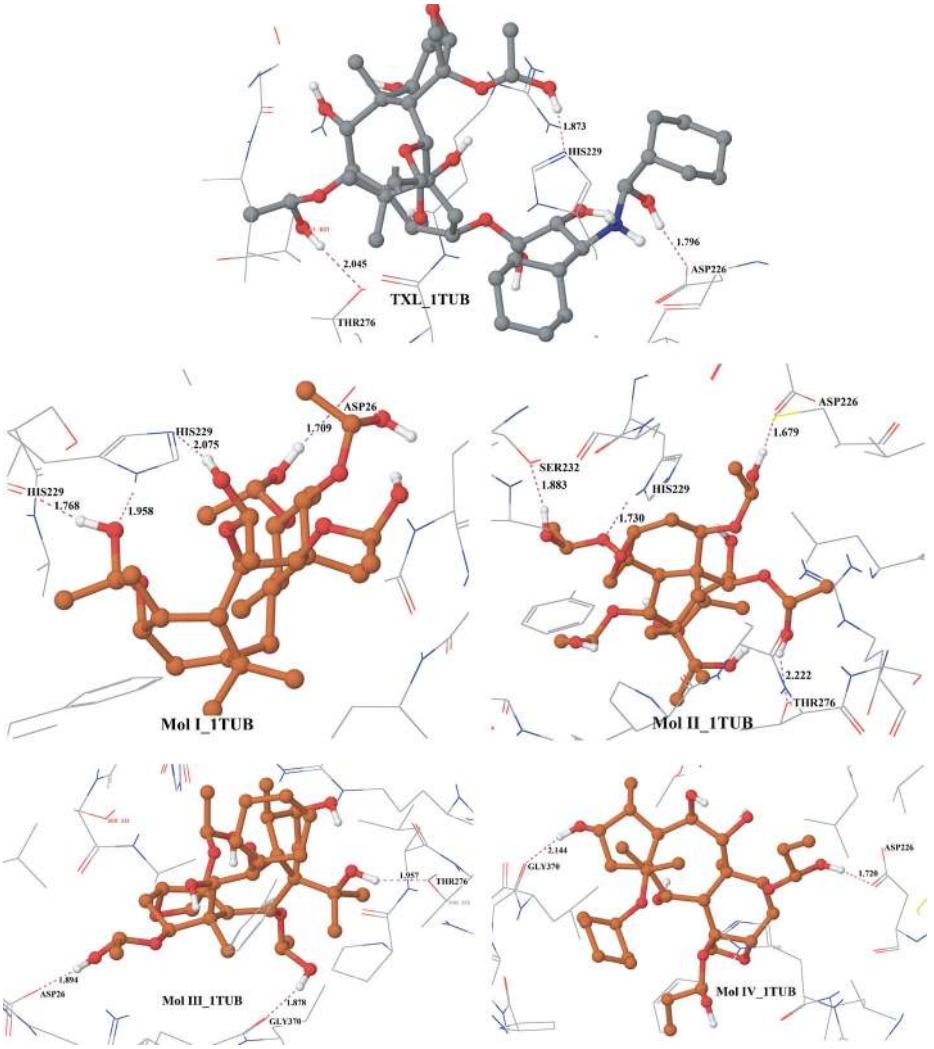

Fig. 2 Hydrogen bonding interactions in the best docking configurations of ligands with tubulin αβ-dimer (1TUB)

O type classical hydrogen bondings are displayed by the ligands within the active site of the protein. It has also been observed that the refined structure of tubulin greatly increases the chances of non-covalent interactions. Taxol exhibits four O-H…O-type and one N-H…O-type interactions involving residues ARG278, THR276, PRO274, ASP26, and GLY370. Molecule IV exhibits four O-H…O and one C-H..N hydrogen bonding interactions with THR276. Residue HIS229 interacts through hydrogen bonding with all the ligands except TXL. Also, residues PRO274, ARG278, and ASP26, etc., are caught up with non-covalent hydrogen bonding interactions with ligands. Since there are no planar rings present in the ligands, as in the previous docking, π-π or cation-π interactions are not observed in the best docking complexes. Hydrophobic and polar interactions are similar, as in the case of docking with 1TUB (Fig. S2).

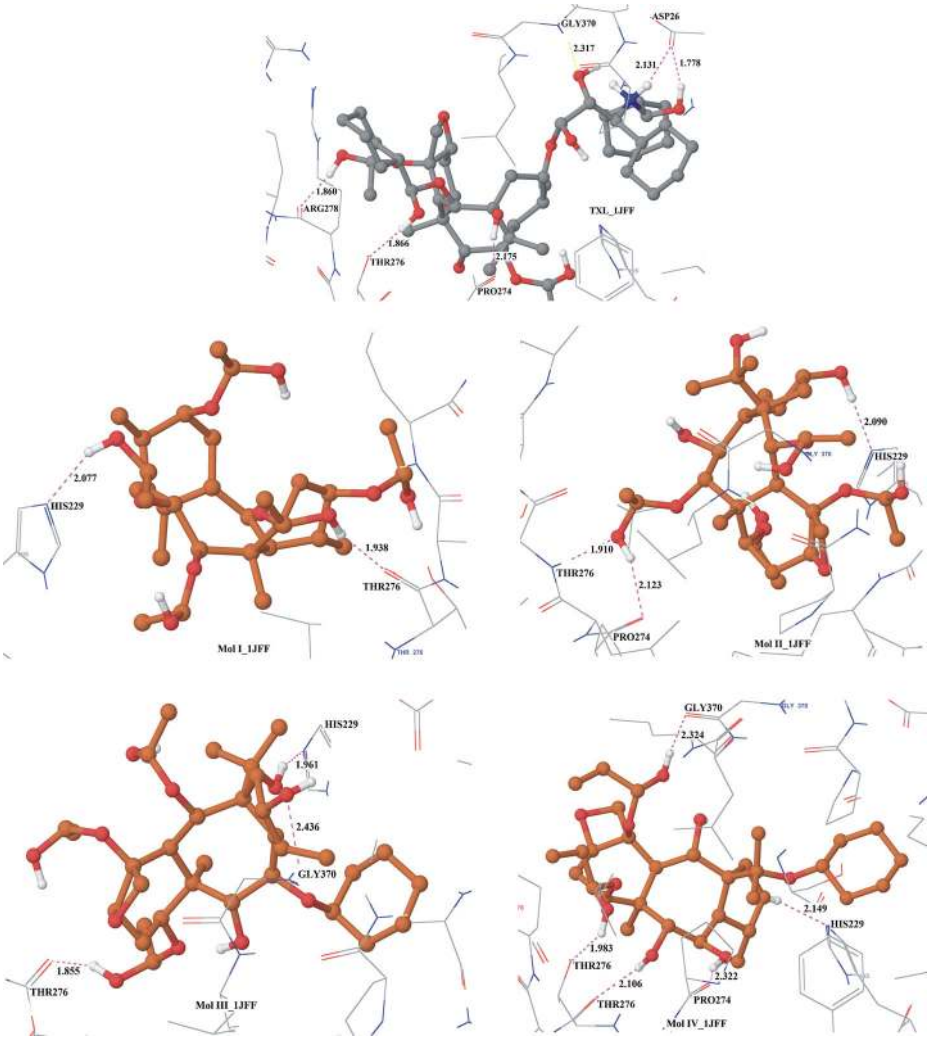

Fig. 3 Hydrogen bonding interactions in the best docking configurations of ligands with refined microtubule structure (1JFF)

Table 4 Comparison of best Glide scores and best Glide energies with experimental inhibitory activities [9] (*NA: experimental data not available)

Compound	Glide score		Glide energy		IC50 value*			
	1TUB	1JFF	1TUB	1JFF	HepG2	A498	NCl-H226	MDR2780AD
I	−11.457	−13.213	−76.004	−79.718	NA	NA	NA	NA
II	−8.633	−7.800	−56.152	−47.111	NA	NA	NA	NA
III	−8.980	−8.158	−58.302	−48.614	124.0	112.0	132.0	156.0
IV	−8.402	−8.046	−55.411	−49.800	68.0	157.0	94.0	182.0
TXL	−8.986	−8.500	−55.251	−40.916	7.4	96.3	61.2	0.19

3.3 Docking of taxol (TXL)

In the case of TXL binding with αβ-tubulin dimer (1TUB), it has been found that the minimum docked energy is −76.004 kcal/mol. The best Glide score is −11.457, corresponding to docked energy −67.812 kcal/mol. The minimum docked energy out of 20 docked configurations of TXL binding with refined structure of tubulin 1JFF has been found to be −79.718 kcal/mol, which corresponds to the docking score of −11.925 kcal/mol. Docking of taxol within the active site of the refined structure of tubulin 1JFF show that the Glide score is enhanced to −13.213 kcal/mol. Hydrogen bonding interactions exhibited by TXL, for the best binding configuration with 1TUB, are O-H…O and N-H…O types involving residues ASP226, HIS229, and THR276. The best docked configuration of TXL with 1JFF demonstrates O-H…O hydrogen bonding with residues ARG278, THR276, PRO274, ASP26, and GLY370, while N-H…O hydrogen bonding with ASP26. Considering the docked energy and interactions, it may be inferred from Tables 1, 2, and 3 and Figs. 2 and 3 that TXL has the best binding capabilities with both 1JFF and 1TUB in comparison to other taxoids.

3.4 Docking of molecule I

Molecule I, a taxane diterpenoid obtained from the needles of *Taxus wallichiana*, has a similar structure to that of TXL except that the long aliphatic chains are replaced by hydroxyl groups. The docking of molecule I with 1TUB reveals the minimum docked energy of −56.152 kcal/mol, with a Glide score of −7.786 kcal/mol. The best docking Glide score for the binding of molecule I with 1TUB is found to be −8.633 kcal/mol. It has the third best binding energy and fourth best Glide score in comparison to the binding of other taxoids considered for the study. The docking complex of molecule I with 1JFF has minimum energy −47.111 kcal/mol, while the minimum Glide score is found to be −7.800 kcal/mol. The best docked complex with 1TUB reveals O-H…O hydrogen bonds with residues HIS229 and ASP26. N-H…O hydrogen bonding is also exhibited in the best docking configuration with residue HIS229. O-H…O and N-H…O hydrogen bonding interactions are shown by molecule I in the best docking configuration with 1JFF with respect to residues HIS229 and THR276. It shows less hydrogen bonding interactions in docking with 1JFF than 1TUB.

3.5 Docking of molecule II

Taxoid II, obtained from the heartwood of *Taxus wallichiana*, whose archetype is taxol, has a seven-membered ring in the core in place of the eight-membered ring system in taxol. The long aliphatic ring system has been replaced by the hydroxyl group, showing a greater tendency for O-H…O hydrogen bonds. Glide Extra-Precision docking of this molecule with 1TUB reveals the lowest binding energy of −58.302 kcal/mol. For the best docked configuration, the Glide score is −8.980, with docked energy −56.868 kcal/mol. Docking with 1JFF exhibits increased magnitude of the best Glide score equal to −8.158 kcal/mol, which is the third best after TXL and molecule IV. On the basis of energy considerations, molecule II has minimum docking energy of −48.614 kcal/mol, which is again the third best energy value after TXL and molecule III. In the docking complex of II with 1TUB, O-H…O type hydrogen bonding interactions are found with residues ASP226, SER232, and THR276, and the complex shows better binding energy and interactions compared to molecules I, III, and IV, but less binding energy and interactions than TXL. Hydrogen bonding interactions exhibited by this molecule with 1JFF are O-H…O-type interactions involving residue PRO274 and N-H…O-type interactions with residue HIS229 and THR276.

3.6 Docking of molecule III

The core rings of the taxoids III and IV are the same as those of compound II, but they differ in having different substituents. Compound III has a greater number of hydroxyl groups, whereas IV has less ionizable hydrogens. Docking of III with 1TUB reveals the docking energy −53.114 kcal/mol for the best docking score −8.402 kcal/mol. The minimum docking energy is found to be −55.411 kcal/mol with docking score of −8.302. On the basis of Glide score, binding energy, and interactions, molecule III shows the fourth best binding capability with 1JFF among the five taxoids. The molecular docking results with 1JFF indicate that the minimum docking energy is −49.800 kcal/mol, which is of lower magnitude than that exhibited with 1TUB. For the best docking configuration of the molecule III_1TUB complex, O-H…O hydrogen bonding exists with residues THR276, ASP26, and GLY370. Docking with 1JFF demonstrates hydrogen bonding interactions in the complexes with residues of the active site THR276, GLY370, and HIS229.

3.7 Docking of molecule IV

Molecule IV has a similar chemical structure to that of molecule III, but with fewer hydroxyl substituents. Molecule IV exhibited the least magnitude of docking energy but the second best Glide score with both microtubules (1TUB and 1JFF). The minimum binding energy for the best docked configuration with 1TUB was found to be −55.251 kcal/mol, with a docking score −8.351 kcal/mol. Docking of molecule IV with 1JFF demonstrates the docking energy in their best docking configurations equal to −40.916 kcal/mol with a docking score −8.500 kcal/mol. The best docking complex of molecule IV with 1JFF has the least binding energy in comparison to other taxoids but the second best Glide score. Comparisons show that compound IV has the least magnitude of binding energy with 1JFF and 1TUB both compared with any other ligands considered under study. Extra-Precision docking of ligand IV with 1TUB exhibits evidence for O-H…O-type hydrogen bonding with ASP226 and GLY370 residues. Hydrogen bonding interactions exhibited by molecule IV with 1JFF are O-H…O and C-H…N types involving residues THR276, PRO274, HIS229, and GLY370.

3.8 Molecular dynamics simulation

To ensure the stability of ligands in the classical taxol binding site and time evolution of the docked complexes, molecular dynamics simulations of the best docked configurations (with 1JFF) of all the ligands were carried out at room temperature for 15.0 ns using DESMOND. It is better to take docking complexes with 1JFF for MD study than 1TUB, as 1JFF is the refined structure of αβ-tubulin dimer with improved resolution. To come within reach of the real situation, MD simulation is performed in water and neutralized with Na^+ counter ions. The average RMSD of heavy atoms of the complexes of the residues during MD simulation are plotted in Fig. 4. It is observed that taxol binding shows small fluctuations in the beginning but takes up an almost constant value of 2.00 Å at 8.0 ns for the rest of dynamics. Average RMSD increases linearly from 0.50 ns to 4.0 ns while very slow increasing behavior is observed from 4.0 ns to 8.0 ns. MD simulation of molecule I complexed with microtubule shows constant RMSD of 2.4 Å up to 7.50 ns, and afterwards then slowly increases to 2.7 Å at the end of 15.0-ns dynamics. MD structure of best docked complex of molecule II quickly transits in the simulation to 2.0 Å RMS deviation with reasonably small oscillations centered around it, throughout the course of dynamics. Molecules III and IV also exhibit fluctuations in the beginning, but RMSDs of their complexes with protein become constant at 2.0 Å and 2.4 Å

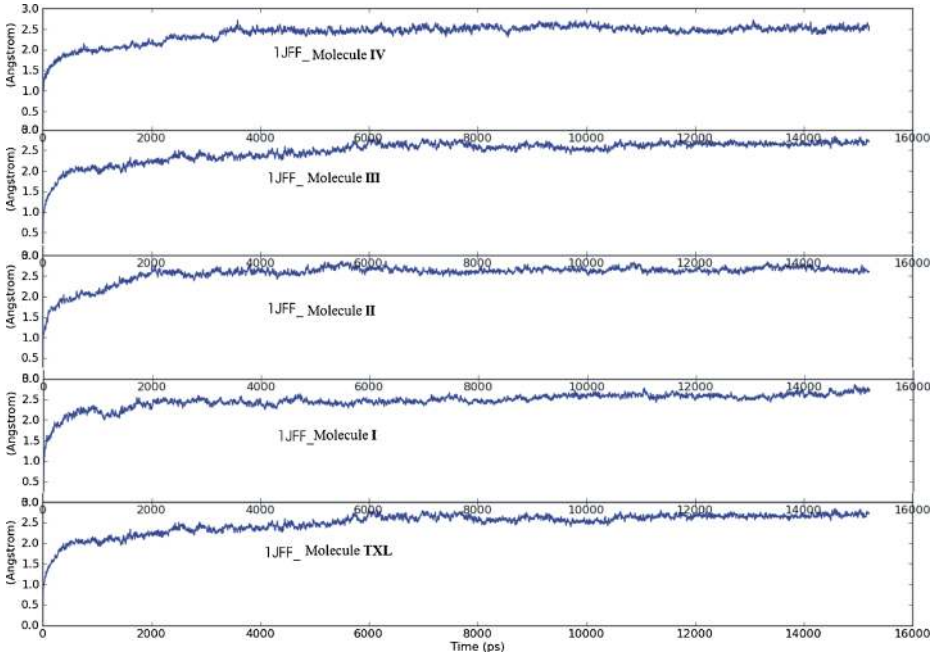

Fig. 4 Average RMSD of heavy atoms of the complexes during MD simulation

during the course of dynamics from 10.5 ns and 4.0 ns, respectively. In saturation state, the range of oscillations of the dynamical structures around the MD average are about ±0.03 Å for each structure. The observed average RMS fluctuations of individual residue positions from their mean positions indicate that the residues ASP226 show very small fluctuations in almost all the structures, representing the possibility of non-covalent interactions with it.

Total solute energy variation of the complexes with simulation time is shown in Fig. 5. The negative binding energy indicates the strong binding of ligand with the receptor. Small fluctuation in total energy indicates that the hydrogen bonding and other non-covalent interactions alternate among the residues of the active site. We have also observed that the main contribution in the total energy comes from the electrostatic energy for all components (receptor, complex, and ligand), while the difference of the van der Waals energy is more negative with respect to the electrostatic energy, which indicates the an optimal configuration of ligand to reach the cavity of receptor. High contributions of the polar group indicate that inhibition of enzyme is mostly supported by the hydrophilic interactions. Total solute energy of molecule IV is reduced suddenly from −60 kcal/mol to −100 kcal/mol at 2.5 ns and remains constant up to 7.4 ns, which again increases to the preceding value, indicating strong hydrogen bonding interactions during 2.5 ns to 7.5 ns. Molecule II exhibits minimum energy value of complex having small fluctuations around −75.0 kcal/mol, throughout the entire course of dynamics.

Protein interactions with the ligands have been monitored all over the simulation. These interactions are shown in Fig. 6. Protein–ligand interactions are categorized into four types; hydrogen bonds, hydrophobic, ionic, and water bridges. The stacked bar charts are normalized over the course of the trajectory. Values over 1.0 are possible, as some protein residues may make multiple contacts of the same subtype with the ligand. A simulation interaction diagram

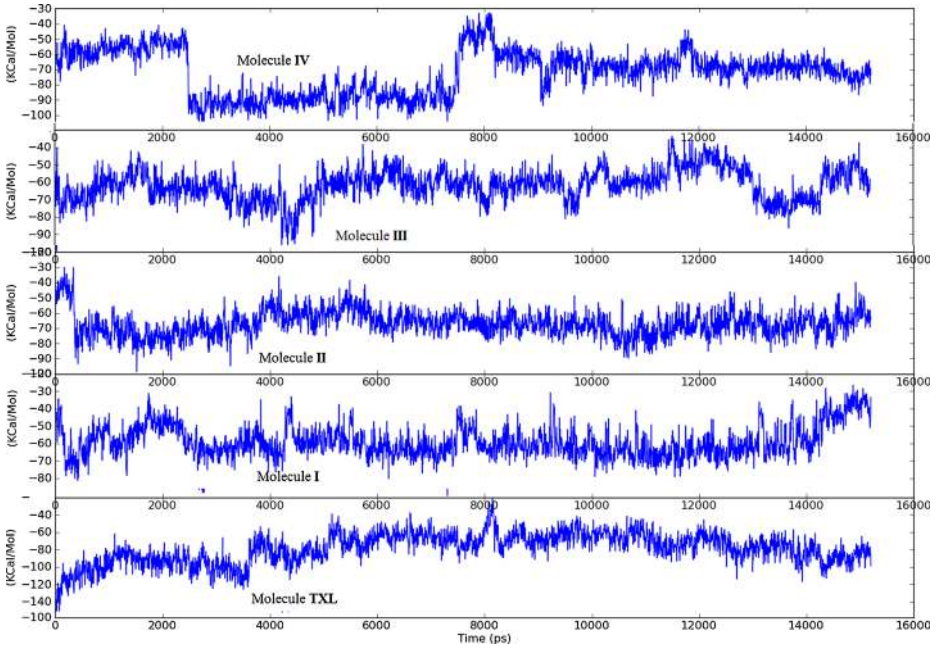

Fig. 5 Variation of total energy of complexes during MD simulation

shows that water bridges play an important role in the binding of taxol, molecule I, and molecule II within the active site while hydrophobic and hydrogen bonding interactions are the

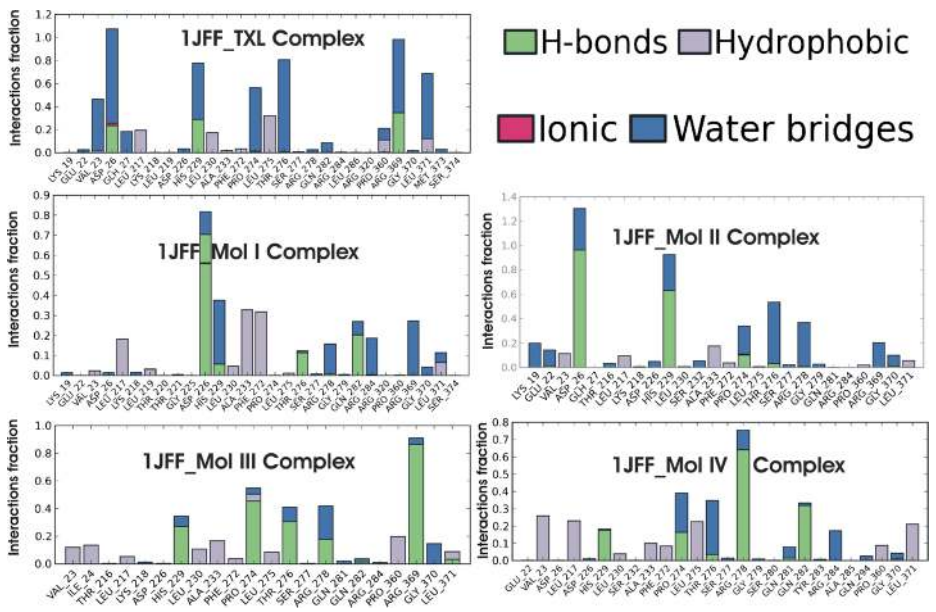

Fig. 6 Normalized stacked bar chart representation of interactions and contacts over the course of trajectory (values over 1.0 are possible as some residue make multiple contacts of same subtype with ligands)

Table 5 Some molecular properties of ligands as obtained through Qikprop MW: Molecular weight; Mol. Vol.: Molecular volume; nRotb: Number of rotatable bonds; nON: Number of hydrogen bond acceptors (O and N atoms); nOHNH: Number of hydrogen-bond donors (OH and NH groups); PSA: Polar surface area; LogP: Octanol-water partition coefficient; Log (S): aqueous solubility; PCaco: Apparent Caco-2 Permeability (nm/sec); nMetab: number of primary metabolites; Abs.: % Human Oral Absorption in GI (±20 %); nViol5: number violations of Rule of 5; nVol3: number of violations of rule of 3

Molecule	M. W.	Mol. Vol.	nRotb	nON	nOHNH	PSA	Log (P)	Log (S)	PCaco	nMetab.	Abs.	nViol5	nViol3
TXL	886.171	2341.408	32.0	22.7	9.5	181.884	1.793	−0.236	29	7	25	3	1
I	576.766	1573.499	15.0	17.0	5.0	118.800	1.092	−1.848	403	0	67	1	0
II	578.696	1521.221	16.0	18.8	7.0	151.407	−0.157	−1.494	229	3	29	3	0
III	616.788	1708.280	19.0	17.1	6.0	131.102	1.567	−2.361	428	6	44	3	0
IV	600.788	1697.251	15.0	15.4	6.0	122.322	2.229	−3.368	591	4	64	2	0
Range of 95 % drugs	130 to 725	500 to 2000	0.0 to 15.0	2.0 to 20	0.0 to 6.0	7.0 to 200.0	−2.0 to 6.5	−6.5 to 0.5	>25	1–8	>25 %	0–4	0–2

main contributors in the case of molecules III and IV. Taxol interacts with residues ASP26 and ARG369 throughout the course of dynamics. Other residues that show prominent interactions with TXL are HIS229, THR276, LEU371, and VAL23. Interactions through hydrogen bonds and water bridges with ASP26 of taxol and molecule II are maintained effectively by 110% and 130% of the simulation time, respectively. HIS229 shows interactions with molecule I for ~96% of the simulation time. Major interactions of molecules III and IV within the active site involve the residues ARG369 and ARG278, respectively.

Small fluctuations in RMSD, total negative energy of the solute complexes, and time line study of interactions and contacts are good indications of system stability. However, molecule II and taxol-binding stability predominates over molecules I, III, and IV.

3.9 ADME/T prediction

The ADME properties inspected using QikProp 3.5 (Table 5) indicate that all the molecules show violations of Lipinski's 'rule of 5' ranging from 1 to 3 but 95 % of these have parameters within the range given in Table 5. Molecules violating more than two or three of these rules may have problems with bioavailability. Molecules I-IV do not exhibit violation of the 'rule of 3'. However, taxol shows one violation of the 'rule of 3'. A compound is viewed as potentially problematic if it does not satisfy a 'rule-of-three': predicted log S>−6, cell permeability >30 nm/s, and maximum number of six primary metabolites. Of the molecules studied, 95% have an octanol-water partition coefficient (LogP) within the range given in Table 5. A higher log (P) value represents poor absorption. Aqueous solubility (Log S), cell permeability (PCaco), and number of primary metabolites are also within the range for all molecules. When studied using Tox-Tree software, taxol was analyzed as highly toxic among all the compounds because it contains some functional groups that are associated with enhanced toxicity. On the basis of ADME/T predictions, it may be inferred that molecules I-IV may have less side effects compared to taxol.

4 Conclusions

Docking studies of the TXL and taxoids I, II, III, and IV with tubulins 1TUB and 1JFF give an idea about the binding energy and interactions within the classical taxol-binding site of the microtubule. Results demonstrate that taxol has better binding capabilities than all the other taxoids undertaken for study. However, ADME/T predictions show that molecules I-IV have lesser side effects than taxol. On the basis of docking energy and interactions, it may be inferred that, apart from TXL, molecule II exhibits better binding capabilities with both 1TUB and 1JFF in comparison to other taxoids. Molecular dynamics simulation of the best docked complexes of ligands with 1JFF indicate that the complexes remain stable during the course of dynamics. However, molecule II and taxol binding stability predominates over molecules I, III, and IV.

Acknowledgments U. Yadava is thankful to the Department of Science and Technology, New Delhi, for the financial support through its Fast Track Young Scientist Scheme and University Grants Commission, New Delhi for the award of Raman Fellowship.

References

1. Pellegrini, F., Bubman, D.R.: Tubulin function, action of antitubulin drugs, and new drug development. Cancer Invest **23**, 264–273 (2005)

2. Kathiravan, G., Sri Raman, V.: In vitro TAXOL production, by *Pestalotiopsis breviseta* — a first report. Fitoterapia **81**, 557–564 (2010)
3. Schiff, P.B., Fant, J., Horwitz, S.B.: Promotion of microtubule assembly in vitro by taxol. Nature **277**, 665–669 (1979)
4. Giannakakou, P., Gussio, R., Nogales, E., Downing, K.H., Zaharevitz, D., Bollbuck, B., Poyi, G., Sackett, D., Nicolaou, K.C., Fojo, T.: A common pharmacophore for epothilone and taxanes: molecular basis for drug resistance conferred by tubulin mutations in human cancer cells. PNAS **97**, 2904–2909 (1999)
5. Wang, H.K., Ohtsu, H., Itokawa, H.: Chemistry of taxol and related taxoids. In: *Taxus*: the genus Taxus, Ed. Itokawa, H. and Lee, K.H. Taylor & Francis, London. p225 (2003).
6. Chattopadhyay, S.K., Sharon, A., Yadava, U., Srivastava, S., Mehta, V.K., Maulik, P.R.: A taxane diterpenoid from the needles of *Taxus wallichiana*. Acta Cryst. **E57**, o1158–o1160 (2001)
7. Chattopadhyay, S.K., Sharon, A., Yadava, U., Srivastava, S., Mehta, V.K., Maulik, P.R.: A taxane diterpenoid from the heartwood of *Taxus wallichiana*. Acta Cryst. **E58**, o154–o155 (2002)
8. Yadava, U., Gupta, H., Roychoudhury, M.: A comparison of crystallographic and DFT optimized geometries on two taxane diterpenoids and docking studies with phospholipase A2. Med. Chem. Res. **21**, 2162–2168 (2012)
9. Khan, I., Nisar, M., Ahmad, M., Shah, H., Iqbal, Z., Saeed, M., Muhammad, S., Halimi, A., Kaleem, W.A., Qayum, M., Amana, A., Abdullah, S.M.: Molecular simulations of Taxawallin I inside classical taxol binding site of β-tubulin. Fitoterapia **82**, 276–281 (2011)
10. Nogales, E., Wolf, S.G., Downing, K.H.: Structure of the αβ tubulin dimer by electron crystallography. Nature **391**, 199–203 (1998)
11. Lowe, J., Li, H., Downing, K.H., Nogales, E.: Refined structure of αβ-tubulin at 3.5 Å resolution. J. Mol. Biol **313**, 1045–1057 (2001)
12. Glide: version 5.8, Schrödinger, LLC, New York (2012).
13. Halgren, T.A., Murphy, R.B., Friesner, R.A., Beard, H.S., Frye, L.L., Pollard, W.T., Banks, J.L.: Glide: a new approach for rapid, accurate docking and scoring. 2. Enrichment factors in database screening. J. Med. Chem. 47, 1750–1759 (2004).
14. Friesner, R.A., Murphy, R.B., Repasky, M.P., Frye, L.L., Greenwood, J.R., Halgren, T.A., Sanschagrin, P.C., Mainz, D.T.: Extra-Precision Glide: docking and scoring incorporating a model of hydrophobic enclosure for protein-ligand complexes. J. Med. Chem. **49**, 6177–6196 (2006)
15. Yadava, U., Singh, M., Roychoudhury, M.: Pyrazolo [3,4-d]pyrimidines as inhibitor of anti-coagulation and inflammation activities of phospholipase A2: insight from molecular docking studies. J. Biol. Phys. **39**, 419–438 (2013)
16. Banks, J.L., Beard, H.S., Cao, Y., Cho, A.E., Damm, W., Farid, R., Felts, A.K., Halgren, T.A., Mainz, D.T., Maple, J.R., Murphy, R., Philipp, D.M., Repasky, M.P., Zhang, L.Y., Berne, B.J., Friesner, R.A., Gallicchio, E.: Levy. R.M.: Integrated Modeling Program, Applied Chemical Theory (IMPACT). J. Comp. Chem. **26**, 1752–1780 (2005)
17. Jorgenson, W.L., Maxwell, D.S., Tirado-Rives, J.: Development and testing of the OPLS all atom force field on conformational energetic and properties of organic liquids. J. Am. Chem. Soc. **118**, 11225–11236 (1996)
18. Sherman, W., Day, T., Jacobson, M.P., Friesner, R.A., Farid, R.: Novel procedure for modelling ligand/receptor induced fit effects. J. Med. Chem. **49**, 534–553 (2006)
19. Li, Y.C., Rissanen, S., Stepniewski, M., Cramariuc, O., Róg, T., Mirza, S., Xhaard, H., Wytrwal, M., Kepczynski, M., Bunker, A.: Study of interaction between PEG carrier and three relevant drug molecules: piroxicam, paclitaxel, and hematoporphyrin. J. Phys. Chem. B **116**, 7334–7341 (2012)
20. Bissantz, C., Folkers, G., Rognan, D.: Protein-based virtual screening of chemical database. 1. Evaluation of different docking/scoring combinations. J. Med. Chem. 43, 4759–4767 (2000).
21. DESMOND Molecular Dynamics System, version 3.1, D. E. Shaw Research, New York, NY (2012).
22. Bowers, K.J., Chow, E., Xu, H., Dror, R.O., Eastwood, M.P., Gregersen, B.A., Klepeis, J.L., Kolossvary, I., Moraes, M.A., Sacerdoti, F.D., Salmon, J.K., Shan, Y. and Shaw, D.E.: Scalable Algorithms for Molecular Dynamics Simulations on Commodity Clusters. Proc. ACM/IEEE Conf. Supercomp.(SC06), Tampa, Florida (2006).
23. Verlet, L.: Computer "experiments" on classical fluids I. Thermodynamical properties of Lennard-Jones molecules. Phys. Rev. **159**, 98–103 (1967).
24. QikProp: version 3.5 Schrödinger, LLC, New York (2012)
25. Lipinski, C.A.: Drug-like properties and the causes of poor solubility and poor permeability. J. Pharmacol. Toxicol. Methods **44**, 235–249 (2000)
26. Jorgensen, W.L., Duffy, E.M.: Prediction of drug solubility from structure. Adv. Drug. Deliv. Rev. **54**, 355–366 (2002)
27. Cramer, G.M., Ford, R.A., Hall, R.L.: Estimation of toxic hazard - a decision tree approach. J. Cosmet. Toxicol. **16**, 255–276 (1978)
28. Srivastava, H.K., Chourasia, M., Kumar, D., Sastry, G.N.: Comparison of computational methods to model DNA minor groove binders. J. Chem. Inf. Model. **51**, 558–571 (2011)